

## Control of Exciton-photon Coupling in GaN-based Microcavities

*Takehiko Tawara<sup>†</sup>, Hideki Gotoh, and Tetsuya Akasaka*

### Abstract

To obtain novel quantum optics devices useful for quantum information technology, we have demonstrated the ability to control both the weak and strong exciton-photon coupling regimes in GaN-based microcavities at room temperature. High-quality microcavities were obtained with a  $Q$  factor as high as 460 by using a new fabrication technique. Lasing action with a low threshold of  $5.1 \text{ mJ/cm}^2$ , which is half the previously reported value, was observed in the weak coupling regime. Moreover, cavity polaritons were formed with anti-crossing dispersion and Rabi splitting of  $6 \text{ meV}$  in the strong coupling regime.

### 1. Introduction

The coupling between light and matter in optical microcavities has been intensively studied with the aim of controlling the properties of the electronic states by controlling the photonic environment surrounding them [1]. The rapid progress in nanofabrication technologies in recent years has enabled us to achieve light-matter coupling in the solid state such as in semiconductor microcavities with quantum wells (QWs). In semiconductor microcavities, excitons in QWs (matter) interact with cavity photons (light). An exciton is a quantized particle composed of an electron-hole pair bound together by Coulomb attraction; a cavity photon has a discrete resonant energy due to a wavelength-sized cavity length. Exciton-photon coupling in semiconductor microcavities yields intriguing physics such as the modification of spontaneous emission and the cavity polariton effect and its bosonic features. Such coherent manipulation of quantum states is a promising approach for developing novel quantum optics devices useful for quantum information technology. The ability to control exciton-photon coupling at room temperature and an understanding of the fundamental physics are important for the implementation of actual devices.

Exciton-photon coupling has two distinct regimes:

(i) the weak coupling regime, where the spontaneous emission rate can be modified and (ii) the strong coupling regime, where the atom-like state of an exciton can couple coherently with the single photon mode; this is discussed in more detail in Sec. 2. In the weak coupling regime, the electronic excitation decays irreversibly, i.e., the photon emitted by the electron-hole recombination of the exciton is not re-absorbed by the same exciton. Moreover, electron-hole recombination is allowed only if its energy matches the energy of the resonant cavity photon. Thus, the spontaneous emission process in the microcavity is modified compared with that in free space, as shown in **Fig. 1(a)**.

On the other hand, the optical properties in the strong coupling regime are quite different from those in the weak coupling regime. Namely, there is reversible decay, where there is an energy exchange between the exciton and photon modes as shown in **Fig. 1(b)**. An exciton emits a photon through the recombination process. After a round-trip to the cavity mirror and back, this photon is re-absorbed by the same exciton, which then emits a photon again. These continuous exchange processes represent strong coupling and produce the mixed exciton-photon state called cavity polaritons. In recent years, much attention has been focused on the behavior of these polaritons as composite bosons. Photons, which are bosons, tend to occupy the same energy state, whereas two electrons, which are fermions, cannot occupy the same state as a consequence of the Pauli exclusion

<sup>†</sup> NTT Basic Research Laboratories  
Atsugi-shi, 243-0198 Japan  
E-mail: tawara@nttbrl.jp

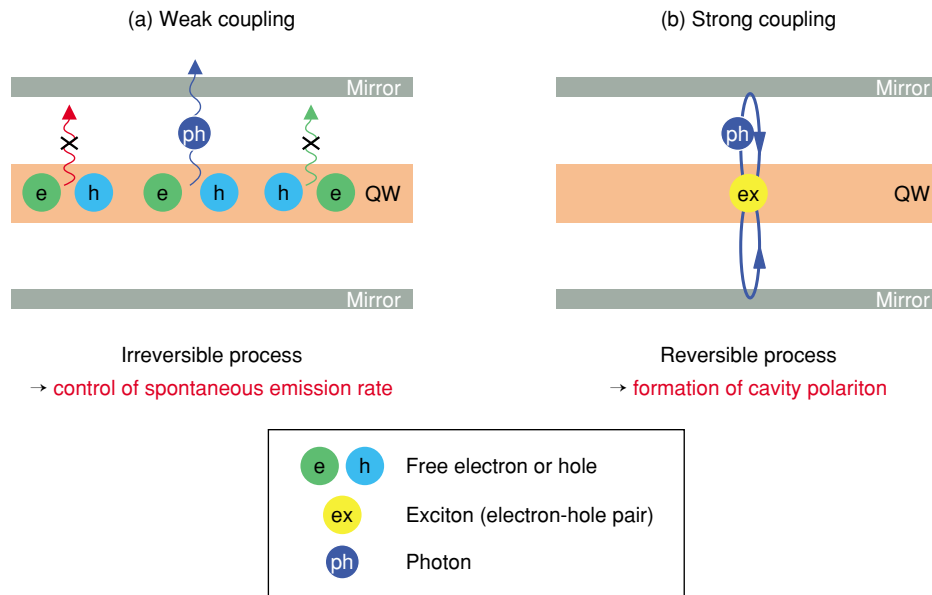


Fig. 1. Schematic explanation of (a) weak and (b) strong exciton-photon coupling in microcavities.

principle. Therefore, polaritons have the potential to produce collective Bose-Einstein condensation (BEC), as observed in atomic systems.

Recently, such exciton-photon coupling in semiconductor microcavities has attracted a great deal of attention as a means of developing novel optical devices for quantum information technology and coherent next-generation light sources such as single photon emitters [2], entangled photon emitters [3], and thresholdless lasers [4]. By using the specific properties of the weak coupling regime mentioned above, we can make optical devices with a high emission efficiency such as vertical-cavity surface-emitting lasers (VCSELs). Moreover, we can expect to make a highly efficient single photon emitter by using a quantum dot embedded in a three-dimensional microcavity as the result of coupling an atomic-like two-level system to a very small mode volume [2].

Polaritons acting as a composite boson in the strong coupling regime exhibit strong parametric scattering due to polariton-polariton interaction, and this parametric fluorescence is predicted to produce strongly correlated photon pairs of signal and idler polaritons [3], [5]. Another topic of interest is related to the BEC of polaritons. These polaritons will condense to their final state with a gain as a result of certain scattering processes; then, unlike in the weak coupling case, coherent light will be emitted from the polaritons in that state without a threshold or any population inversion [4].

GaN-based semiconductors are promising materi-

als for making microcavity systems. It is well known that the excitons in GaN-based semiconductors have a larger oscillator strength and larger binding energy than those in conventional compound semiconductors such as GaAs [6]. Therefore, GaN-based microcavities should exhibit outstanding properties not only in the weak exciton-photon coupling regime but also in the strong coupling regime even at room temperature. Several research groups have attempted to fabricate GaN-based microcavity structures using monolithically grown GaN/AlGaIn distributed Bragg reflectors (DBRs) [7]. However, it was difficult to obtain high-quality microcavity structures that could reach the strong coupling regime because of the lattice-mismatch in GaN-based DBRs. If we are to control the exciton-photon coupling in GaN-based microcavities, we must first achieve strong coupling at room temperature by using high-quality microcavities.

This paper reports the control of exciton-photon coupling in GaN-based QW microcavities at room temperature. Section 2 describes the theory and experimental prospects of exciton-photon interaction in microcavities. Section 3 describes the fabrication of high-quality GaN-based microcavity structures. Experimental results related to the optical properties of weak and strong exciton-photon coupling are discussed in Sec. 4. Particular attention is paid to the formation of polaritons as a result of strong exciton-photon coupling, which was achieved for the first time in GaN-based microcavities at room temperature.

## 2. Exciton-photon interaction in microcavities

A typical microcavity structure is shown schematically in **Fig. 2**. It consists of a planar Fabry-Pérot cavity with QWs sandwiched between two DBRs. In this case, a QW exciton state, with a well-defined transverse  $k$  momentum ( $k_{//}$ ), is coupled to a single cavity-

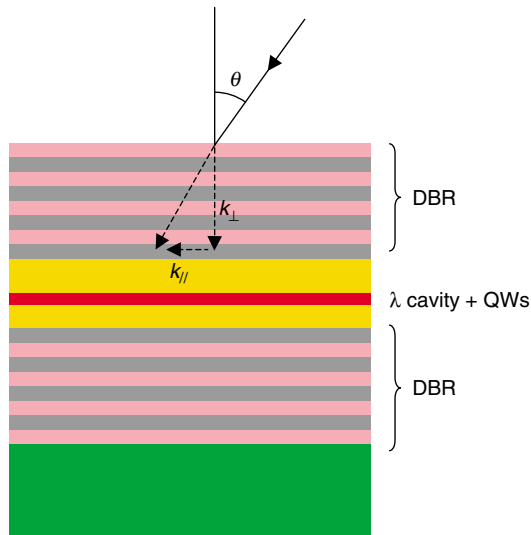


Fig. 2. Typical structure of one-dimensional semiconductor microcavity. Dotted arrows show the transverse ( $k_{//}$ ) and longitudinal ( $k_{\perp}$ ) wavevectors of the photon inside the cavity.

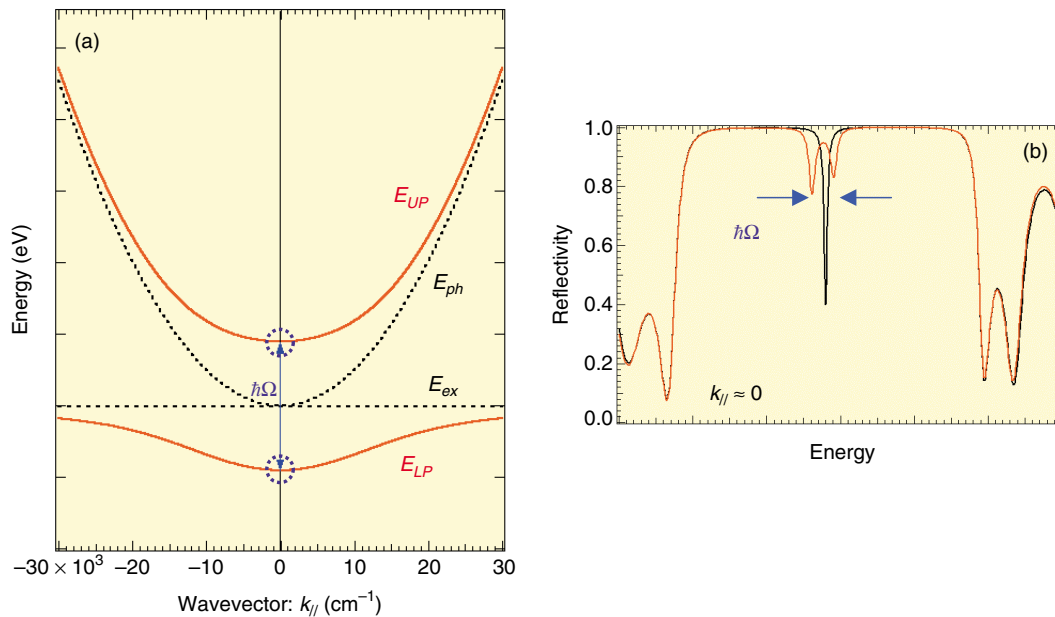


Fig. 3. (a) Dispersion relationship of the cavity photon ( $E_{ph}$ ) and QW exciton ( $E_{ex}$ ), shown by dotted black curves. Red curves show the dispersion relation of the upper polariton ( $E_{UP}$ ) and lower polariton ( $E_{LP}$ ) branches with strong coupling. Rabi splitting is denoted by  $\hbar\Omega$ . (b) Reflection spectra in weak (black curves) and strong (red curves) coupling regimes at  $k_{//} \approx 0$ .

photon mode with the same in-plane wave vector due to momentum conservation caused by the in-plane translational invariance of the electronic and photonic systems. Therefore, we need to consider only the  $k_{//}$  values of the photon and exciton.

The energy dispersion relationships for a cavity photon and QW exciton with various  $k_{//}$  values (dotted curves) are shown in **Fig. 3(a)**. If the excitons are embedded in a microcavity, then an energy exchange between the exciton and photon, known as Rabi oscillation, appears in principle. The Rabi oscillation frequency  $\Omega$  is given by [8]

$$\Omega = 2\hbar \sqrt{g(f)^2 - \left(\frac{\gamma_{ex} - \gamma_{ph}}{4}\right)^2}, \quad (1)$$

where  $\gamma_{ex}$  ( $\gamma_{ph}$ ) is the exciton (photon) linewidth and  $g(f)$  is a coupling factor whose square is proportional to the exciton oscillator strength  $f$ . This coupling factor is given by

$$g(f) = \left[ \frac{2\pi}{\epsilon_r} \frac{1}{4\pi\epsilon_0} \frac{e^2 N f}{m L_{eff}} \right]^{1/2}, \quad (2)$$

where  $\epsilon_r$  ( $\epsilon_0$ ) is the relative (vacuum) permittivity,  $e$  ( $m$ ) is the electron charge (mass),  $N$  is the oscillator density coupled to the cavity mode, and  $L_{eff}$  is the effective cavity length.

If the excitons are bleached by strong excitation or if the coupling factor is smaller than the linewidth term in Eq. (1), the system switches to the weak coupling regime, i.e., Rabi oscillation does not occur. However, in this regime the spontaneous emission rate, i.e., the coupling efficiency to the cavity mode, is modified compared with that in free space. The spontaneous emission rate given by Fermi's golden rule is proportional to  $Q/V$ , where  $Q$  is the quality factor of the cavity mode and  $V$  is the mode volume. In the case of a microcavity,  $Q$  can be increased and  $V$  can be decreased by designing the DBR reflectivity and the cavity length appropriately. Therefore, we can expect high emission efficiency when a microcavity is used in the weak coupling regime. The coupling efficiency of the spontaneous emission was investigated experimentally to measure the dependence of the integrated emission intensity on the excitation power.

In contrast, if the coupling factor is much larger than the linewidth term in Eq. (1), the system maintains strong coupling. In this regime, an anti-crossing mixed state with a Rabi frequency is formed as upper and lower polariton branches, as shown by the red curves in Fig. 3(a). This Rabi frequency value reflects the strength of the exciton-photon coupling and should be proportional to  $(f)^{1/2}$ , as shown in Eqs. (1) and (2), when the linewidth contrast can be assumed to be  $\gamma_{ex} - \gamma_{ph} \approx 0$ . Therefore, we can expect the exciton-photon coupling to be enhanced by an increase in the oscillator strength coupled to the cavity mode. Rabi oscillation also appears as spectral splitting and is known as vacuum-field Rabi splitting  $\hbar\Omega$  in the wavelength domain, as shown by the red curve in Fig. 3(b). These spectral dips correspond to upper and lower polaritons. The formation of these polaritons in the strong coupling regime is confirmed by the appearance of such dips in the reflection spectra.

### 3. Fabrication of InGaN QW microcavities

We used high-quality GaN-based microcavities to control the exciton-photon interaction. They were fabricated using a wafer bonding technique with a GaN-based QW layer and dielectric DBRs (Fig. 4(a)) [9]. The  $4\lambda$ -thick InGaN/AlGaIn QW layers ( $\lambda$ : wavelength) were grown directly on n-type 6H-SiC substrates by metalorganic vapor phase epitaxy. The QW consisted of three or ten sets of 5-nm-thick  $\text{In}_{0.02}\text{Ga}_{0.98}\text{N}$  barriers and 2.5-nm-thick  $\text{In}_{0.15}\text{Ga}_{0.85}\text{N}$  active layers with an  $\text{Al}_{0.07}\text{Ga}_{0.93}\text{N}$  buffer layer. The QWs were placed at the anti-node position of the res-

onant optical wave in the cavity. We removed the SiC substrate from the InGaN QW layer using a conventional dry etching technique. After removing the substrate, we sandwiched the QW layer between  $\text{SiO}_2/\text{ZrO}_2$  DBRs deposited on sapphire substrates using a wafer-bonding technique. We could freely control the refractive index and thickness of the bonding layer. In this study, the design values for refractive index and thickness were 1.5 and 200 nm, respectively. The maximum reflectivity of the bare  $\text{SiO}_2/\text{ZrO}_2$  DBR was about 99% at 400 nm with a 100-nm-wide stopband. A cross-sectional image taken with a scanning electron microscope is shown in Fig. 4(b). This image shows that we were able to obtain a high-quality GaN-based microcavity structure without surface roughening or cracks.

## 4. Experimental results and discussion

### 4.1 Weak coupling regime

To investigate the optical properties of the fabricated microcavities in the weak coupling regime, we measured the emission spectra under a high excitation condition at room temperature [9]. The optical pump source was a  $\text{YVO}_4/\text{LBO}$  laser emitting 10-ns-wide pulses at a wavelength of 355 nm with a repetition rate of 20 kHz. The excitation beam was incident normal to the sample surface and focused with an objective lens to a spot diameter of 21  $\mu\text{m}$ . The spontaneous emission spectrum from the InGaN microcavity at room temperature is shown in Fig. 5(a). We observed narrow emission at 400 nm. Its peak position and width both corresponded to those of the cavity resonance mode observed by reflection measurement. In this wavelength range, the full width at half maximum (FWHM) of this emission was 0.87 nm, which gave a  $Q$  factor of 460. It should be noted that the resolution limit of our spectrometer was 0.06 nm in this wavelength region. Using this  $Q$  factor, we estimated the effective reflectivity of the DBRs to be about 98%, which is almost equal to the maximum reflectivity of the bare DBRs (99%).

We measured the emission intensity dependence on the optical excitation power in this microcavity at room temperature. We accumulated a series of emission intensities for 104 pulses and plotted them as a function of excitation energy per pulse (Fig. 5(b)). This figure shows a clear threshold at an excitation energy  $E_{\text{th}}$  of 17.5 nJ/pulse. Lasing occurred at a wavelength of 401 nm, as seen in Fig. 5(c). This threshold energy of 17.5 nJ/pulse corresponds to an energy density of 5.1 mJ/cm<sup>2</sup>. We also observed spec-

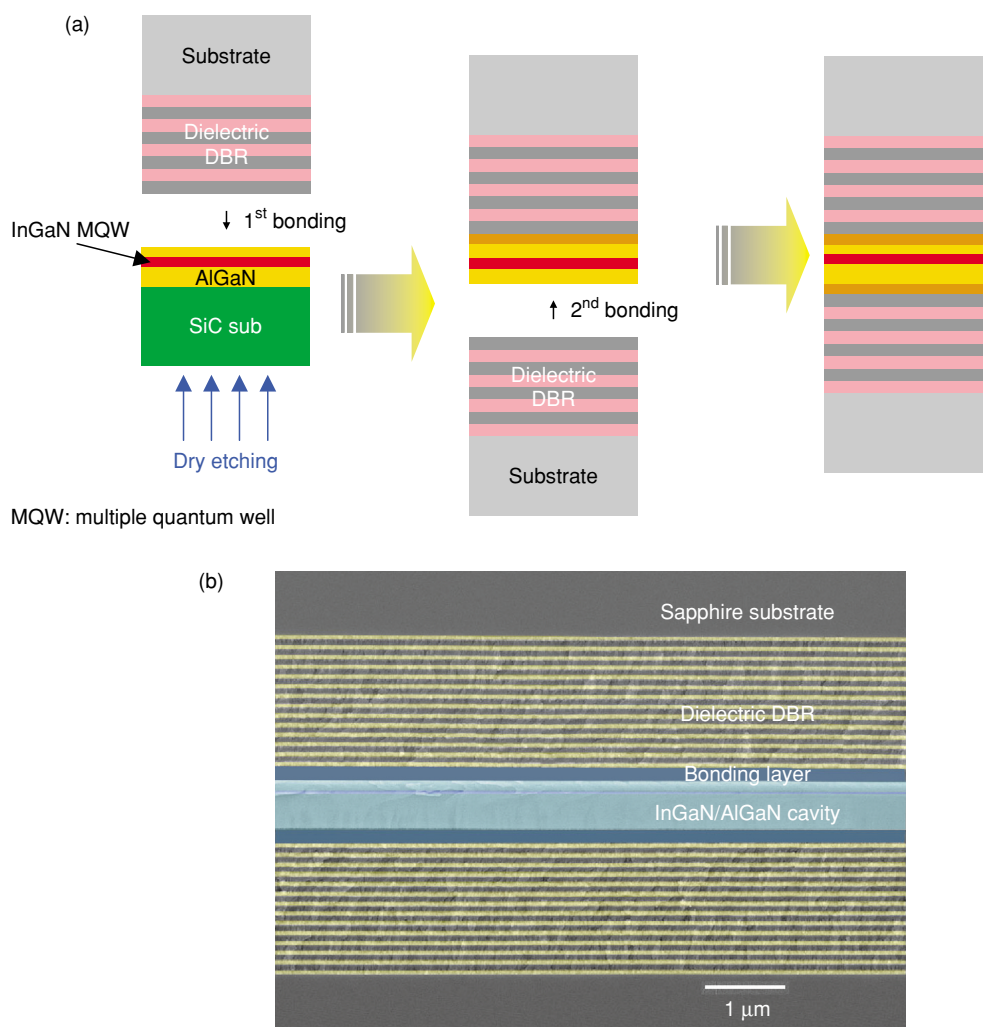


Fig. 4. (a) Schematic diagram of the fabrication of an InGaN microcavity after removal of the SiC substrate from the cavity layer, which is sandwiched between dielectric DBRs. (b) Cross-sectional image taken with a scanning electron microscope.

tral narrowing above the threshold, as shown in Fig. 5(c), and the lasing FWHM was about 0.2 nm.

From these lasing properties, we could calculate the spontaneous emission factor ( $\beta$ ) in the InGaN microcavities. This factor indicates the coupling efficiency of the spontaneous emission to the lasing mode, and it increases as the cavity mode volume decreases. **Figure 5(d)** shows the emission intensities of 3QW cavity in Fig. 5(b), replotted on a logarithmic scale. The difference in emission intensity before and after lasing corresponds to  $\beta$  of about  $10^{-2}$ . This means that the spontaneous emission in this microcavity is coupled to the lasing mode 1000 times as effectively as in typical edge-emitting lasers with a  $\beta$  of about  $10^{-5}$  [10].

Someya *et al.* reported room-temperature lasing in

GaN cavities with InGaN QWs at a threshold density of  $10 \text{ mJ/cm}^2$  with hybrid DBRs [7]. The lasing of our microcavities was achieved at a threshold energy density of  $5.1 \text{ mJ/cm}^2$ , which is half the value reported in Ref. 6. This was due to the high-quality crystalline cavity and QW layers that were grown directly on SiC substrates without surface roughening or cracking. These results may help to make possible both low-threshold VCSELs and highly effective single photon emitters based on GaN semiconductors. Moreover, they suggest that strong coupling can be achieved in GaN-based microcavities.

#### 4.2 Strong coupling regime

Next, we examined the optical properties of our microcavities in the strong coupling regime. For this

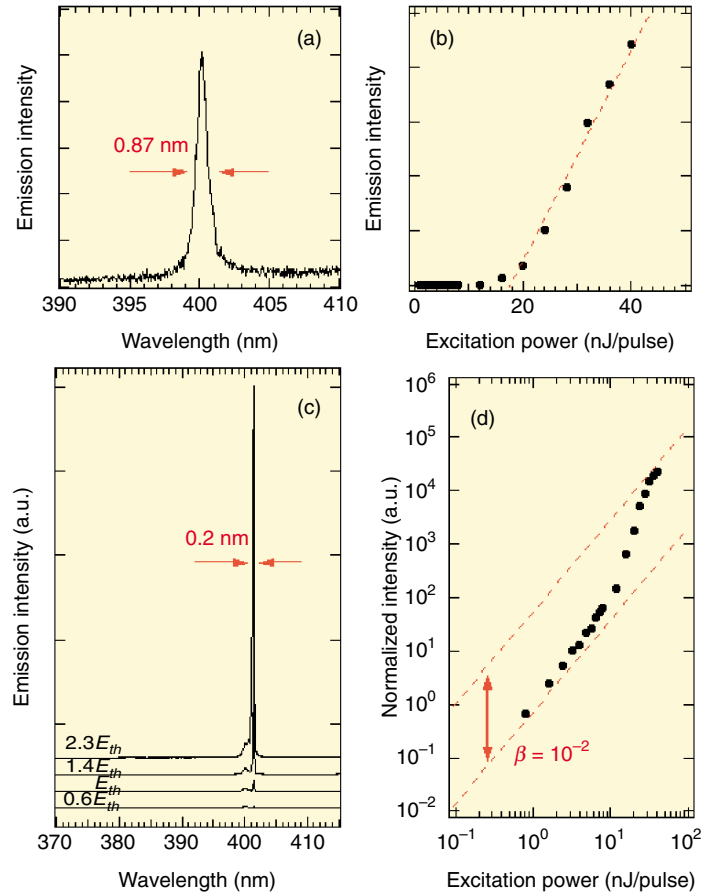


Fig. 5. Optical properties in weak coupling regime. (a) Spontaneous emission spectrum, (b) dependence of the emission intensity on optical excitation power, (c) emission spectra at various excitation powers, and (d) emission intensities of 3QW cavity in (b) re-plotted on a logarithmic scale. Integrated intensities were normalized by that at the lowest excitation energy.

purpose, we measured the reflection spectra using the cavity detuning method at room temperature [11]. We used a Xe lamp focused with an objective lens as the optical light source and we limited its effective spot size on the sample surface to about  $20\ \mu\text{m}$  by using a pinhole. The light was incident normal to the sample surface. The GaN-based cavities were formed in a wedge-like shape where the energy of the cavity mode varied spatially at a rate of  $0.2\ \text{meV}/\mu\text{m}$ . The reflection spectra of the empty cavity (without QWs) are shown in **Fig. 6(a)**. These spectra were obtained using a probe light at intervals of  $200\ \mu\text{m}$  along the sample surface. It can be clearly seen that the cavity resonance position could be controlled linearly. We achieved a  $Q$  factor as high as 400 in this cavity, which corresponds to an FWHM ( $\gamma_{ph}$ ) of 7 meV.

The reflection spectra of the QW microcavities for various degrees of cavity detuning are shown in **Fig. 6(b)**. We observed the appearance and disappearance

of splitting at positions around 2.807 eV and these positions varied with the cavity detuning energy  $\delta = E_{ph} - E_{ex}$ , where  $E_{ph}$  is the cavity mode energy and  $E_{ex}$  is the InGaN exciton energy. In this case,  $E_{ex}$  was assumed to be 2.807 eV. These dip position energies are shown as a function of  $\delta$  in **Fig. 6(c)**. In this figure, the anti-crossing behavior is clearly revealed by the vacuum-field Rabi splitting of 6 meV caused by cavity detuning, where the Rabi splitting value reflects the strength of the exciton-photon coupling.

The red curve in Fig. 6(b) is a theoretical dispersion curve for the Rabi splitting calculated from the multiple-interference analysis obtained with a DBR Fabry-Pérot interferometer using a transfer matrix for optical propagation. The measured linewidth of the cavity mode  $\gamma_{ph}$  was 7 meV. The fitting parameters in this calculation were the Lorentzian homogeneous linewidth of the InGaN exciton  $\gamma_{ex}$  and the peak absorption coefficient  $\alpha$ . Values of  $\gamma_{ex} = 15\ \text{meV}$  and

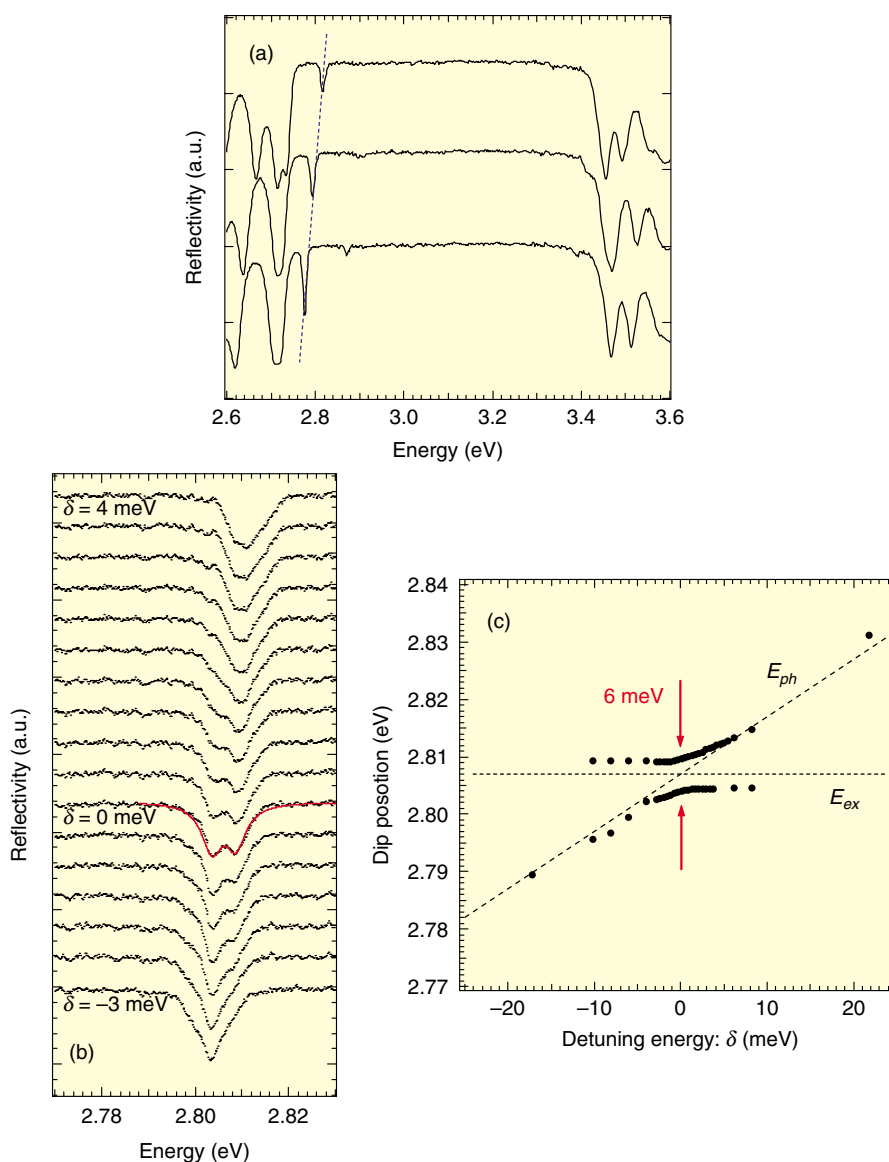


Fig. 6. (a) Reflection spectra of empty cavity measured at various positions at room temperature. (b) A series of reflection spectra of InGaN QW microcavities for various degrees of cavity detuning  $\delta = E_{ph} - E_{ex}$ . The red curve shows the calculated spectrum. (c) The dip positions in (b) plotted as a function of the detuning energy  $\delta$ .

$\alpha = 4 \times 10^5 \text{ cm}^{-1}$  yielded good agreement between the theoretical curves and the experimental results. This value of  $\alpha$  is of the same order of magnitude as that for GaN QW excitons [12]. Using these parameters, we deduced that  $Nf = 2.0 \times 10^{13} \text{ cm}^{-2}$  per QW. For reference, GaAs QW microcavities have been reported to have  $Nf = 4.8 \times 10^{12} \text{ cm}^{-2}$  per QW [13]. The oscillator strength of InGaN QW excitons is one order of magnitude larger than that of GaAs QW excitons.

To prove that polaritons were formed in the strong coupling regime, we must observe the dependence of the polariton dispersion on  $k_{//}$ . We measured the

angle-resolved photoluminescence (PL) spectra of the fabricated cavities at room temperature. The optical pump source was the second harmonic of a Ti-sapphire laser emitting 10-ns-wide pulses at 355 nm with a repetition rate of 5 kHz. In this study, the PL spectra were measured under a non-resonant excitation condition, i.e., the samples were excited outside the cavity stopband. The wavevector of the light through a DBR differs depending on the direction of the emission. A dispersion image of the PL emissions from the microcavities obtained by angle-resolved PL measurements at room temperature is shown in

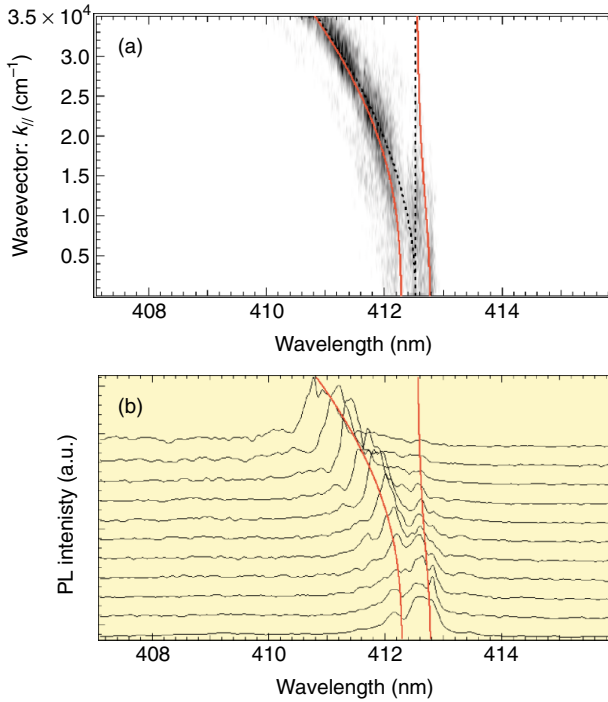


Fig. 7. Angle-resolved PL spectra measured at room temperature. (a) CCD image of the dispersion curve of the polaritons. Red and dotted curves show the calculated dispersion curve of polaritons and uncoupled mode, respectively. (b) Series of the PL spectra with various  $k_{||}$ .

**Fig. 7(a)**, and the spectrum for each value of the wavevector in it is shown in **Fig 7(b)**. Two split branches, which correspond to lower and upper polariton branches, can be seen with a Rabi splitting of 6 meV, which is the same as the reflection value.

The dispersions of the cavity photon ( $E_{ph}$ ), QW exciton ( $E_{ex}$ ), and polariton ( $E_{pol}$ ) are given by

$$E_{ph}(k_{||}) = \frac{\hbar c}{n_{cav}} \sqrt{\left(\frac{2\pi}{L_{cav}}\right)^2 - k_{||}^2}$$

$$E_{ex}(k_{||}) = E_{ex}(0) + \frac{\hbar^2 k_{||}^2}{2M_{ex}} \quad (3)$$

$$E_{pol}(k_{||}) = \frac{E_{ph} + E_{ex}}{2} \pm \sqrt{g^2 - \frac{(E_{ph} - E_{ex})^2}{4}},$$

where  $n_{cav}$  and  $L_{cav}$  are the refractive index and length of the cavity, respectively, and  $M_{ex}$  is the effective mass of the exciton. In Fig. 7(a), the dotted and red curves show the dispersions  $E_{ph}$ ,  $E_{ex}$ , and  $E_{pol}$  calculated using the parameters. These calculations con-

sidered the actual cavity structure and used an estimated oscillator strength of  $2.0 \times 10^{13} \text{ cm}^{-2}$  per QW. The theoretical curves of  $E_{pol}$  reproduced the experimental results well. These results also reveal the formation of an InGaN polariton in the luminescence.

Our InGaN QWs in the as-grown samples had a PL linewidth of about 200 meV. Note that this linewidth is the sum of the homogeneous and inhomogeneous linewidths in the QW emission. It is well known that the In composition of an InGaN QW fluctuates in the QW plane. The light emission from the InGaN QW originates from localized excitons in the In-rich regions and this leads to inhomogeneous spectral broadening [14]. When the localized excitons in an InGaN QW have discrete energy states such as excitons in quantum dots, only those excitons whose energy matches the cavity resonant energy contribute to the strong coupling. The amount of Rabi splitting is determined by the homogeneous linewidth at the exciton energy [15]. This is generally disadvantageous for strong coupling compared with the situation in a homogeneous QW where all the excitons can couple to the cavity mode. In our InGaN QW microcavities, however, the localized excitons with large oscillator strengths at certain discrete energy levels enabled us to observe the Rabi splitting. Moreover, such a localized exciton effect appeared in the angle-resolved PL measurements, as shown in Fig. 7. In these results, the luminescence from the upper polariton branch is stronger than that from the lower branch in the  $k_{||} \gg 0$  region. This is due to two exciton states with different transition energies coupling to a cavity mode with different detuning energies. Therefore, the upper branch forms a hybrid state, and its density of states increases effectively. Achieving strong coupling in GaN-based microcavities is an important step in the investigation of fundamental polaritonic physics at room temperature. Moreover, it will lead to polaritonic devices based on bosonic behavior such as entangled photon emitters and thresholdless lasers operating at room temperature.

## 5. Conclusion

This paper described the control of the exciton-photon interaction in GaN-based QW microcavities at room temperature. High-quality microcavities were obtained with a  $Q$  factor as high as 460 by using selective etching and wafer bonding techniques. In these fabricated microcavities, low-threshold lasing of  $5.1 \text{ mJ/cm}^2$ , half the previously reported value, was observed in the weak coupling regime. These micro-

cavities also exhibited an enhanced spontaneous emission rate of 1000 times those of conventional edge-emitting lasers. Moreover, a strong exciton-photon interaction was achieved at room temperature. Cavity detuning and angle-resolved measurements confirmed the anti-crossing behavior of the cavity polaritons with a vacuum-field Rabi splitting of 6 meV. Until now, strong coupling and bosonic behavior of polaritons have been examined only at low temperatures using GaAs-based microcavities. At higher temperatures, many scattering processes for polaritons such as phonon scattering are believed to exist. These process collapse polaritons and prevent bosonic behavior. The bosonic behavior of the polaritons should open up new scientific fields such as coherent manipulation of bosons in the solid state and lead to a new generation of optical devices. The results described here should play an important role in clarifying these scattering mechanisms at room temperature and finding solutions to these problems. This will lead to novel quantum optics devices that will be useful for quantum information technology.

## References

- [1] See, e.g., E. Burstein and C. Weisbuch, "Confined electrons and photons," NATO Advanced Science Institute Series B, Vol. 340, Italy, 1993.
- [2] G. S. Solomon, M. Pelton, and Y. Yamamoto, "Single-mode spontaneous emission from a single quantum dot in a three-dimensional microcavity," *Phys. Rev. Lett.*, Vol. 86, p. 3903, 2001.
- [3] C. Cui, "Branch-entangled polariton pairs in planar microcavities and photonic wires," *Phys. Rev. B*, Vol. 69, p. 245304, 2004.
- [4] A. Imamoglu, R. J. Ram, S. Pau, and Y. Yamamoto, "Nonequilibrium condensates and lasers without inversion: Exciton-polariton lasers," *Phys. Rev. A* 53, p. 4250, 1996.
- [5] P. G. Savvidis, J. J. Baumberg, R. M. Stevenson, M. S. Skolnick, D. M. Whittaker, and J. S. Roberts, "Angle resonant stimulated polariton amplifier," *Phys. Rev. Lett.*, Vol. 84, p. 1547, 2000.
- [6] G. Malpuech, A. D. Carlo, A. Kavokin, J. J. Baumberg, M. Zamfirescu, and P. Lugli, "Room-temperature polariton lasers based on GaN microcavities," *Appl. Phys. Lett.*, Vol. 81, p. 412, 2002.
- [7] T. Someya, R. Werner, A. Forchel, M. Catalano, R. Cingolani, and Y. Arakawa, "Room temperature lasing at blue wavelength in gallium nitride microcavities," *Science*, Vol. 285, p. 1905, 1999.
- [8] V. Savona, L. C. Andreani, P. Schwendimann, and A. Quattropani, "Quantum well excitons in semiconductor microcavities: Unified treatment of weak and strong coupling regimes," *Solid State Commun.*, Vol. 93, p. 733, 1995.
- [9] T. Tawara, H. Gotoh, T. Akasaka, N. Kobayashi, and T. Saitoh, "Low-threshold lasing of InGaN vertical-cavity surface-emitting lasers with dielectric distributed Bragg reflectors," *Appl. Phys. Lett.*, Vol. 83, p. 830, 2003.
- [10] See, e.g., H. Yokoyama and S. D. Broson, "Rate equation analysis of microcavity lasers," *J. Appl. Phys.*, Vol. 66, p. 4801, 1989.
- [11] T. Tawara, H. Gotoh, T. Akasaka, N. Kobayashi, and T. Saitoh, "Observation of cavity polaritons in InGaN microcavities at room temperature," *Phys. Rev. Lett.*, Vol. 92, p. 256402, 2004.
- [12] A. J. Fischer, W. Shan, J. J. Song, Y. C. Chang, R. Horning, and B. Goldenberg, "Temperature-dependent absorption measurements of excitons in GaN epilayers," *Appl. Phys. Lett.*, Vol. 71, p. 1981, 1997.
- [13] R. Houdré, C. Weisbuch, R. P. Stanley, U. Oesterle, P. Pellandini, and M. Ilegems, "Measurement of cavity-polariton dispersion curve angle-resolved photoluminescence experiments," *Phys. Rev. Lett.*, Vol. 73, p. 2043, 1994.
- [14] Y. Narukawa, Y. Kawakami, S. Fujita, S. Fujita, and S. Nakamura, "Recombination dynamics of localized excitons in  $\text{In}_{0.20}\text{Ga}_{0.80}\text{N}-\text{In}_{0.05}\text{Ga}_{0.95}\text{N}$  multiple quantum wells," *Phys. Rev. B*, Vol. 55, p. R1938, 1997.
- [15] R. Houdré, R. P. Stanley, and M. Ilegems, "Vacuum-field Rabi splitting in the presence of inhomogeneous broadening: Resolution of a homogeneous linewidth in an inhomogeneously broadened system," *Phys. Rev. A*, Vol. 53, p. 2711, 1996.



### Takehiko Tawara

Optical Science Research Laboratory, NTT Basic Research Laboratories.

He received the B.S. degree in applied physics from Nihon University, Tokyo in 1996 and the M.S. and Ph.D. degrees in engineering from Hokkaido University, Hokkaido in 1998 and 2001, respectively. He joined NTT Basic Research Laboratories in 2001. Since then, he has engaged in the study of semiconductor nanostructure fabrication and optical characterization of semiconductor quantum systems. He received the 2000 Young Scientist Award from the Japan Society of Applied Physics (JSAP). He is a member of JSAP.



### Hideki Gotoh

Senior Research Scientist, Optical Science Research Laboratory, NTT Basic Research Laboratories.

He received the B.S., M.S., and Ph.D. degrees in engineering from Hiroshima University, Hiroshima in 1991, 1993, and 2000, respectively. Since joining NTT Basic Research Laboratories in 1993, he has been working on optical physics and device applications of semiconductor nanostructures. He is the member of JSAP and the Optical Society of America.



### Tetsuya Akasaka

Research Scientist, Materials Science Laboratory, NTT Basic Research Laboratories.

He received the B.S., M.S., and Ph.D. degrees in engineering from Tokyo Institute of Technology, Tokyo in 1991, 1993, and 1996, respectively. He joined NTT Basic Research Laboratories in 1996. Since then, he has working on crystal growth and optical device application of nitride semiconductors. He is the member of JSAP.